In *2023 IEEE/RSJ International Conference on Intelligent Robots and Systems* (IROS 2023), Detroit, MA, USA October 2023

A Novel Control Law for Multi-joint Human-Robot Interaction Tasks While Maintaining Postural Coordination

Keya Ghonasgi[1], Reuth Mirsky[2,3], Adrian M. Haith[4], Peter Stone[2,5], Ashish D. Deshpande[1]

***Abstract*— Exoskeleton robots are capable of safe torque-controlled interactions with a wearer while moving their limbs through pre-defined trajectories. However, affecting and assisting the wearer's movements while incorporating their inputs (effort and movements) effectively during an interaction remains an open problem due to the complex and variable nature of human motion. In this paper, we present a control algorithm that leverages task-specific movement behaviors to control robot torques during unstructured interactions by implementing a force field that imposes a desired joint angle coordination behavior. This control law, built by using principal component analysis (PCA), is implemented and tested with the Harmony exoskeleton. We show that the proposed control law is versatile enough to allow for the imposition of different coordination behaviors with varying levels of impedance stiffness. We also test the feasibility of our method for unstructured human-robot interaction. Specifically, we demonstrate that participants in a human-subject experiment are able to effectively perform reaching tasks while the exoskeleton imposes the desired joint coordination under different movement speeds and interaction modes. Survey results further suggest that the proposed control law may offer a reduction in cognitive or motor effort. This control law opens up the possibility of using the exoskeleton for training the participating in accomplishing complex multi-joint motor tasks while maintaining postural coordination.**

I. INTRODUCTION

Recent advances in the design and control of robots have made them safer and more suitable for direct human interaction. A prominent application of physical human-robot interaction (HRI) is to affect and assist human movement through exoskeleton robots. These devices are worn directly on the human body and are being studied for various applications including movement assistance, physical rehabilitation, and performance augmentation. Researchers have shown that impedance control, which is built upon direct control of the joint torques, allows exoskeletons to be safe for human interaction [1]. However, how to assist and affect the wearer's behavior through a shared control of effort and movement remains an open challenge [2]. High-level control laws are necessary to modulate the robot's joint torques in response to the wearer's input while simultaneously achieving the desired movement-based tasks with the robot. Further, such a control law will have to be immune to a lack of knowledge of how, where, and when the wearer may move within the device. For example, does the wearer initiate movement at their wrist or their upper arm? Is the movement speed consistent? This variability in human movement behavior poses an unstructured interaction environment. This paper proposes a control law that aims to accomplish movement-constrained tasks while allowing an individual to comfortably drive an exoskeleton under various interaction conditions whilst maintaining desirable joint coordination.

To enable the exoskeleton's responsiveness using torque control while ensuring the wearer's comfort, the robot must interpret and translate the wearer's movements into appropriate robot joint torques. Human motor control research has shown that humans often perform complex limb movements by coordinating their joints for a given task goal. For example, Bockemuhl et al. [3] showed that individuals coordinated the joints in their arms for different reaching movements. Similar coordination behaviors are observed in upper limb [3], [4], lower limb [5], and dexterous hand movements [6]. Maintaining joint coordination behaviors may also ensure safe interactions between an exoskeleton and its wearer [7], and aid a physical therapist in moving the robot to assist the wearer. In prior work, we demonstrated how joint angle coordination may characterize motor learning over time [8]. Lora et al. [9] presented various methods of coordination-based exoskeleton control for lower-limb exoskeletons. These prior works motivate our goal of implementing a coordination-based control law that imposes a reference joint coordination behavior on the exoskeleton's joints as the wearer drives the robot's movements.

Assuming a joint-angle coordination behavior can be prescribed for a given task, the exoskeleton's control still needs to account for the variability in the wearer's movements. Predicting the user's target motion can inform the exoskeleton's control. However, such predictive methods may either ignore the functional task goal, thereby making interpretation of movement intention difficult [10] or restrict the movement goals to specific tasks, like hand gestures [11] or a single-joint movement [12], to achieve accurate prediction. For functional task assistance, it's important to consider how information encoded within task-specific movements can be used to simplify robot control. Previous implementations of task-assistive control have tested timed trajectories in joint-angle space to assist the wearer's motion. These trajectory-based interactions can have unintended effects due to a mismatch between the wearer's intention and the prescribed motion [13]. The wearer performing the task in the exoskeleton may start their movement at different interface points

[1]Mechanical Engineering Department at The University of Texas at Austin keya.ghonasgi@utexas.edu, ashish.deshpande@austin.utexas.edu

[2]Computer Science Department at The University of Texas at Austin pstone, reuth@cs.utexas.edu

[3]Computer Science Department at Bar Ilan University

[4]Neuroscience Department at Johns Hopkins University adrian.haith@jhu.edu

[5]Sony AI

(e.g. wrist handle or upper arm attachment) or even at a joint that is not directly interacting with the robot. Further, the coupling between the wearer's movement and the exoskeleton may be more consistent at the physical interfaces but weaker where the exoskeleton is expected to actively match the wearer's movements [14]. Finally, in rehabilitation, the robot may need to be driven externally by a physical therapist assisting the wearer with their task such that the interaction is no longer being driven at the interface points. To account for these variabilities, the exoskeleton must use its own sensors and match the desired posture at the relevant joints without relying on explicit information about the expected external interactions. We test the feasibility of our proposed control law for human-exoskeleton interaction under variable input conditions while maintaining task-specific joint-angle coordination behaviors.

Kinematic coordination has been used for defining robot control in the past. Brokaw et al. [15] used a predefined coordination behavior for the joints of the ARMin III robot for time-independent functional training (TIFT) such that one robot joint drives another to maintain coordination. The complementary limb motion estimation (CLME) method by Vallery et al. [16] uses joint angle information from one leg to estimate the movement of the other leg. When implemented on a lower-limb exoskeleton [17], this approach assumes that part of the exoskeleton drives the motion while the rest is driven by the coordination. Finally, in prior work with the Harmony exoskeleton [7], the authors define a non-linear kinematic relationship to maintain natural shoulder girdle coordination known as the scapulohumeral rhythm. In all three cases, the exoskeleton responds to inputs at the driving joints thereby constraining the interaction locations and only allowing partial control of the exoskeleton.

Crocher et al. [18] address this problem of simultaneous coordination of joints by exploiting PCA to define a desired joint velocity synergy and imposing the coordination through a viscous force field. This approach, called Kinematic Synergy Control (KSC), imposes joint velocity coordination rather than postural control in the joint angle space. As a consequence, though the robot's joint velocities are constrained, the joint angles need not be constrained as rigidly. Depending on initial conditions and movement speeds, the robot's joint will accumulate errors and deviate from the desired joint angle coordination over time. This variability is evidenced by a participant's ability to perform different reaching movements with the same joint velocity coordination as presented in [18]. While joint velocity coordination may have its own applications in exoskeleton control, our goal in this paper is to achieve task-specific postural control to allow comfortable movement assistance for the wearer. Thus, in order to coordinate the joint angles of the exoskeleton, we present and implement a novel control law called Joint Angle Coordination Control (JACC) that 1) imposes a pre-defined joint angle coordination behavior, and 2) allows the wearer to drive the exoskeleton without prescribing interaction points and time-dependent expectations.

II. METHODS

The following subsections introduce the proposed control law and the methods used to test its robustness and feasibility.

A. Coordination-Based Controller Design

1) Reference Coordination Identification: We begin by first defining task-specific time-independent joint angle coordination behaviors. Consider a set of reference joint angle signals for a given task θ_{task} of size $T \times n$ where T is the number of time-steps of data collected for the movement, and n is the number of degrees of freedom of the robot. Principal component analysis (PCA) allows the signals to be split into a time-dependent signal matrix S and a time-independent orthonormal coordination matrix C,

$$\theta_{task} = SC^T + \theta_{mean} \tag{1}$$

In this paper, we assume that a desired coordination C_{des} and task mean θ_{ref} are calculated from a reference trajectory, θ_{task} using PCA. S_{des} necessarily satisfies the equation

$$S_{des} = (\theta_{task} - \theta_{mean})C_{des} \tag{2}$$

Note that the matrix C_{des} calculated from the task data is of size $n \times n$ where n is the number of degrees of freedom of the human-robot system. PCA further gives us the primary principal component of the movement which describes the majority of the variability in the movement as the first column of C_{des}. The columns of C_{des} are ordered by how much of the signal variability they capture. The system's dynamics can be reduced by selecting the first m columns where $1 \leq m \leq n$. When $m = n$, the control law described below will not constrain the motion at all. For any $m < n$, the exoskeleton will impose joint angle coordination. When $m = 1$, as in the case presented in this paper, the coordination is restricted to a single line as described in Section II-A.3. The goal of the control law presented in this manuscript is to restrict the movement coordination only to this first principal component referred to as $C_{des,1}$. The reduced system can be written as

$$S_{des,1} = (\theta_{task} - \theta_{mean})C_{des,1} \tag{3}$$

2) Joint Angle Coordination Control: An impedance-controlled force field is used to impose the desired coordination behavior at each joint. The torque commands for the joint angle coordination control (JACC) are

$$\tau_{JACC} = K(\theta_{des} - \theta). \tag{4}$$

Given an arbitrary $\theta(t)$ at time t, we aim to identify the desired joint angles θ_{des} such that the desired joint coordination behavior, $C_{des,1}$ is maintained. At time t, we identify the 1-dimensional time-dependent signal relative to desired coordination $S_{des}(t)$ as

$$S_{des}(t) = (\theta(t) - \theta_{ref})C_{des,1} \tag{5}$$

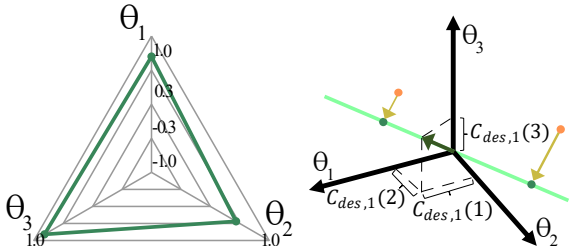

(a) Example 3-dof coordination. (b) Force field visualization.

Fig. 1: Visualizing the control law: Fig. 1a shows an example set of coordination weights $C_{des,1}$ for a 3-dof robot. Fig. 1b shows the coordination unit vector and the corresponding coordination line. The JACC force field brings the robot's joints from non-coordinated configurations to the nearest coordinated point. The yellow arrows represent the error $(\theta_{des} - \theta_{meas})$ that drives the impedance control.

Given S_{des}, θ_{ref}, and C_{des}, the desired joint angles using Eq. 1 are

$$\theta_{des} = (\theta(t) - \theta_{ref})C_{des,1}C_{des,1}^{T} + \theta_{ref} \tag{6}$$

Note that if C_{des} of size $n \times n$ is used in Eq. 5, the corresponding θ_{des} in Eq. 6 is the same as $\theta(t)$. By reducing the dimensionality of C_{des}, we restrict the relative behaviors at each joint to a specific coordination. The calculated desired joint angles θ_{des} define the closest joint angle pose such that the desired coordination is satisfied.

3) Visualization of JACC Force Field: We present a 3-degree of freedom (dof) robot as an example to help visualize the JACC force field. Consider a task performed by this 3-dof robot such that the movement mean is zero, or the measured θ_{ref} is centered around $0_{3\times3}$. Using PCA, we can then identify the corresponding matrix C_{des} and the first principal coordination, $C_{des,1}$, represented in the spider plot in 1a. The corresponding weights of each of the 3 joints of the robot form a unit vector shown in dark green Fig. 1b. Extending this vector infinitely in both directions gives a representation of every coordinated point where the robot's joints satisfy the desired behavior.

When the robot's joints are coordinated per this line, the robot will not move unless acted upon. Consider the case where a user drives the robot arbitrarily causing the instantaneous coordination of the joints to shift to one of the red points in Fig. 1b. The JACC force field identifies the nearest point θ_{des} on the line and, through impedance control, brings the joints of the robot to this desired coordinated configuration. The same correction would occur if one or many joints of the robot are driven simultaneously. This force-field implementation is applicable to any multi-dimensional system with the force-field designed to impose either only the first principal coordination or more depending on the application. As the joint angle behavior is coordinated, the joint velocities of the robot will also be coordinated, with small errors due to the time delay of velocity measurement. However, when joint velocities are coordinated, joint angle coordination cannot be guaranteed in the same way.

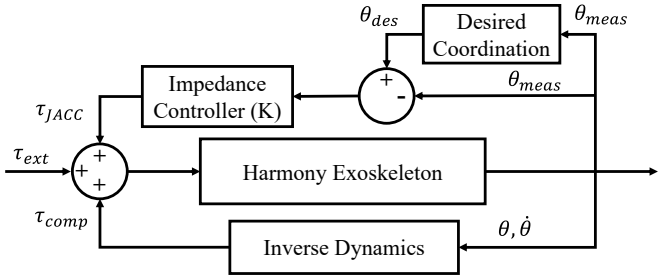

Fig. 2: Control diagram for the Harmony exoskeleton [19].

Note that this implementation of the force field is not possible if the robot's underlying control law is position control. Position control would restrict the robot's movements rigidly to the coordination line, making it difficult and potentially unsafe for an individual to move a joint of the robot independently. Harmony's underlying high-speed torque control facilitates impedance control which allows an individual to move a joint of the robot out of a coordinated pose potentially causing a shift in the nearest point on the coordination line. Further, the stiffness value of the impedance control (K in Eqn. 4) can be changed to modulate how rigidly the robot adheres to the desired coordination. This stiffness modulation is an important parameter of the JACC force field, and we investigate its effect on the robustness and feasibility of the control law for human-exoskeleton interaction.

4) Implementation for the Harmony Exoskeleton: In this paper, we implement the JACC force field for the Harmony exoskeleton, a bi-manual upper-body rehabilitation robot. The robot's control framework, depicted in Fig. 2, applies a compensation torque (τ_{comp}) that accounts for the robot's mass without compensating for inertia or friction effects. In the original control scheme proposed for the exoskeleton [19], the robot maintains the scapulohumeral rhythm (SHR), a non-linear coordination behavior that couples the joints in the shoulder girdle to ensure natural movements. In this paper, we replace this SHR coordination with the linear task-specific reference coordination behavior described above. The joint angles observed by the robot's encoders are passed to the JACC control law described in Eq. 6 to set the desired joint angles. τ_{ext} in Fig. 2 refers to the external torques applied by the wearer as they interact with the robot.

When the robot is in its equilibrium configuration ($\theta_{meas} = \theta_{des}$), and there is no disturbing τ_{ext}, the commanded τ_{JACC} is zero, and the robot continues to compensate for its own weight. As a result, the robot will not move from this configuration. As an individual interacts with the robot, they apply an external torque at some of the robot's joints causing a change in θ_{meas}. Eq. 6 is used to evaluate the new θ_{des} and the impedance controller commands τ_{JACC} to move the robot's joints to the nearest equilibrium configuration.

B. Robustness to Interaction

The control law presented in this paper is expected to constrain and coordinate the robot's movements in joint position space. In this section, we validate the robustness of the control law proposed above by testing the implementation

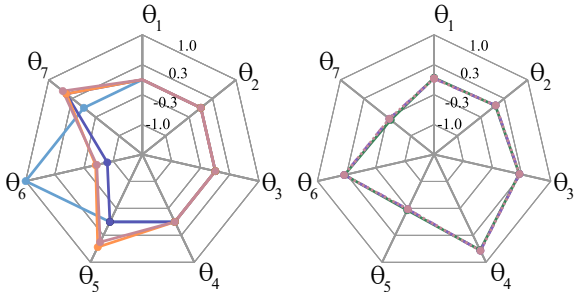

(a) Imposed Coordinations. (b) Testing with Coordination 6.

Fig. 3: Robustness testing: Fig. 3a plots the relative weights of the vectors described in Table I (1 , 2 , 4 , 5). Fig. 3b shows the relative weights of desired and measured coordination behaviors observed when testing coordination vector 6 (stiffness level 1 , and 0.5).

for different types of joint-coordination behaviors against various levels of external perturbation. In particular, we use 6 different coordination behaviors and two levels of virtual stiffness values described in Table I. A stiffness level of 1 refers to the optimally tuned stiffness that allows safe and stable movement of the robot and a level of 0.5 refers to these stiffnesses being halved in the implementation.

The JACC force field is implemented on the Harmony exoskeleton for one 7-dof arm. A desired coordination is represented by a 7×1 vector. The first vector in Table I only allows elbow flexion/extension while locking the other joints to the predefined reference mean angles θ_{ref} set to the nominal home position. The coordination vectors can be visualized using spider plots seen in Fig. 3. In each case, the coordinated joints (with non-zero components in the coordination vector) are manually perturbed through their range of motion. As far as possible, the perturbations are performed independently at each joint during testing.

C. Feasibility for Human-Robot Interaction

The goal of the JACC is to impose joint angle coordination behaviors on human-robot interactive movements. In this section, we test the feasibility and effect of using this coordination-based control on a static reaching task using the Harmony exoskeleton (Fig. 4a).

A total of 7 participants volunteered for this study. The Harmony exoskeleton is first fitted to each participant. Next, the participant is asked to perform a reference straight-line movement reaching from a 'home' position to two different 'target' positions (Fig. 4b). The Harmony exoskeleton is run in the gravity-support mode where it accounts for its own weight but does not account for inertial effects. The participant is provided a visual guide to ensure straight-line motion. The desired coordination vector and reference joint angle mean are constructed for both target-reaching motions for each participant. The participant attempts to perform the same straight-line reaching motions back and forth twice without the visual guide while varying the target (two target positions), reaching speed (0.16Hz, 0.25Hz, and 0.5Hz), and impedance stiffness (1, 0.5, and 0). The condition with 0

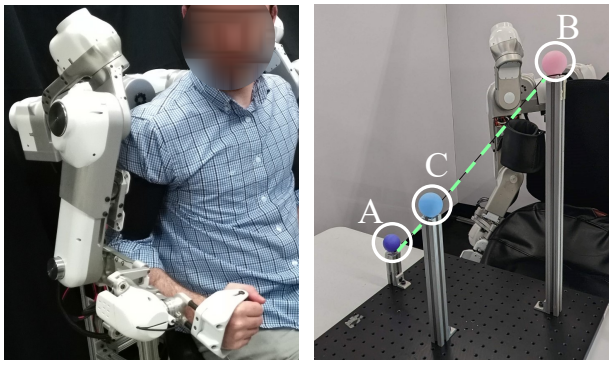

(a) Harmony Exoskeleton. (b) Experiment Setup

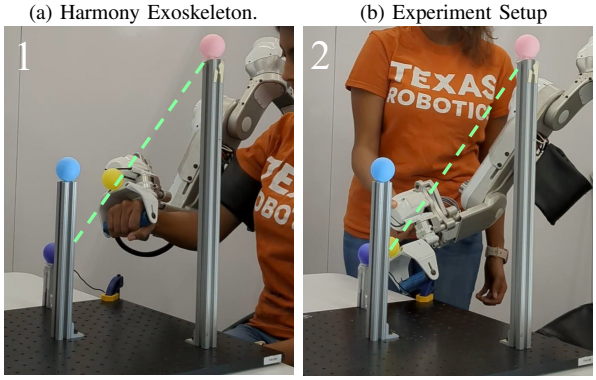

(c) Interaction Conditions

Fig. 4: Experimental setup feasibility testing: Fig. 4a shows the Harmony exoskeleton. Fig. 4b shows the target locations with a black string providing visual feedback for straight-line motion. Individuals perform two straight-line movements, from target A to B, and from target A to C. Fig. 4b shows the "Wear" and "Push" cases in panels 1 and 2 respectively, where the participant either wears or externally pushes the exoskeleton. The string is only used to define the reference coordination (Fig. 4b) and not during testing (Fig. 4c).

stiffness is equivalent to the robot's gravity support mode and is treated as the baseline performance with no assistance from the exoskeleton. To ensure the wearer's safety in the 0-stiffness level, the SHR coordination is imposed [7] in the shoulder. Participants perform 2 repetitions of the reaching movements under two interaction conditions: 1) while wearing the robot, and 2) while holding the robot's wrist actuator from behind the robot (Fig. 4c) in randomized order. This study is conducted with approval from the Internal Review Board at the University of Texas at Austin (STUDY 1215).

By varying the target locations, we inherently vary the desired joint coordination behavior thereby testing robustness for different task conditions. Allowing participants to perform the task at different speeds demonstrates that the control law is effective regardless of the speed of the task performed and does not require prior knowledge of the expected interaction. As participants can perform the task while wearing the robot or while pushing the robot, we further test the robustness and feasibility of the implementation to unknown interactions from a user. Finally, by modulating the impedance stiffness, we test the efficacy of the control law as the force field is strengthened or weakened.

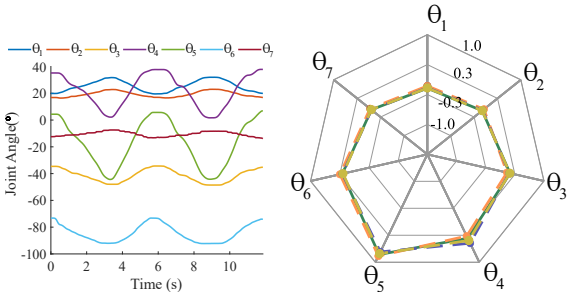

(a) Joint Angles. (b) Coordination Results.

Fig. 5: Representative human-exoskeleton interaction results: Fig. 5a shows the joint angle behaviors in the target reaching task for a representative participant when going from target A to target B with stiffness level 1. Fig. 5b shows the observed coordination behaviors for different stiffness levels where the participant is wearing the exoskeleton and performing the reaching movement at the slowest speed. The solid green line shows the imposed coordination. The dashed lines show the measured joint angle coordination for the 1, 0.5, and 0 levels of stiffness respectively.

III. RESULTS

This section presents the results of the robustness and feasibility experiments for our proposed control law. For each test condition, we use the measured joint angle signals from the exoskeleton to identify the principal components of the movement. The observed joint coordination matrix C_{meas} is then compared against the desired coordination C_{des} using the kinematic coordination distance (KCD) metric [8],

$$D_{P_{des},P_{meas}} = min_{i,j} sin(\phi_{i,j}) = min_{i,j} \sqrt{(1-(u_i \cdot v_i)^2} \quad (7)$$

A KCD of 0 suggests the measured coordination is exactly the same as the desired one, whereas a value of 1 suggests the two coordinations are orthogonal to one another. KCD between vector #1 and #2 in Table I is 0.5.

A. Robustness to Interaction

In general, the KCD between measured and desired coordination behaviors is less than 0.1 for each of the coordination behaviors tested per Table I. This result demonstrates

#	Coordination Vector	Stiffness	KCD
1	$(0,0,0,0,0,1,0)^T$	1	0.01
2	$(0,0,0,0,0,-0.866,0.5)^T$	1	0.05
2	$(0,0,0,0,0,-0.866,0.5)^T$	0.5	0.09
3	$(0,0,0,0,0,0.5,-0.866)^T$	1	0.03
3	$(0,0,0,0,0,0.5,-0.866)^T$	0.5	0.06
4	$(0,0,0,0,0.6245,-0.6,0.5)^T$	1	0.04
4	$(0,0,0,0,0.6245,-0.6,0.5)^T$	0.5	0.08
5	$(0,0,0,0,0.5,-0.6245,0.6)^T$	1	0.03
5	$(0,0,0,0,0.5,-0.6245,0.6)^T$	0.5	0.06
6	$(0.04,0.08,0.28,0.7,-0.29,0.38,-0.43)^T$	1	0.04
6	$(0.04,0.08,0.28,0.7,-0.29,0.38,-0.43)^T$	0.5	0.16

TABLE I: The listed coordination behaviors are imposed using either optimum (1) or halved (0.5) stiffness relative to the tuned full parameters. The KCD column shows the distance between the measured and imposed coordination.

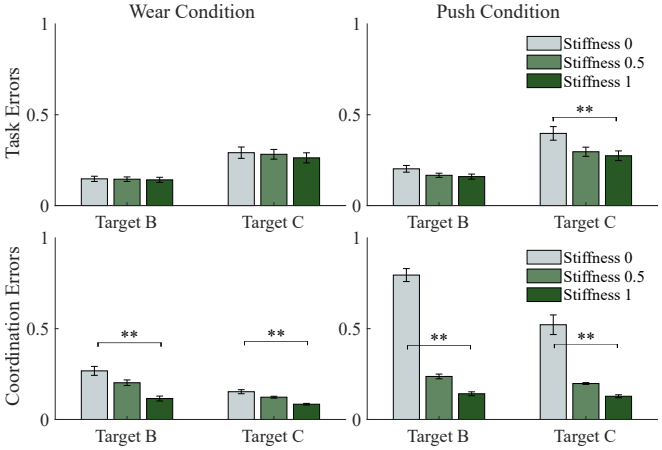

Fig. 6: Task error (first row) and joint angle coordination error (KCD) from the imposed coordination (second row) averaged across participants and movement speeds for three levels of force field stiffness (0, 0.5, 1) and two target motions for the 'wear' (left) and 'push' (right) conditions. '*': $p < 0.05$, '**': $p < 0.01$.

that the control law indeed restricts joint-space coordination behaviors. In addition, we observe that in cases where the impedance stiffness is lower than full stiffness, the corresponding KCD increases. Thus, modulating this stiffness allows control of how rigidly the desired coordination is imposed on the robot's movements.

B. Feasibility for Human-Robot Interaction

The experimental protocol described earlier is used to evaluate how weakly the exoskeleton is able to maintain the desired coordination behavior as an individual interacts with the robot in an unknown and unstructured manner. The movement behavior from one representative participant can be seen in Fig. 5. The measured joint angle signals shown in Fig. 5a for the full stiffness force field are used to evaluate the measured joint coordination behavior shown in Fig. 5b. The KCD to desired coordination for the 1, 0.5, and 0 stiffness levels are 0.06, 0.14, and 0.14 respectively.

The averaged results for the KCD results are shown in Fig. 6. Using repeated measures ANOVA on the data from conditions where participants 'wear' the exoskeleton, we find that regardless of the target position and movement speed, the KCD of measured exoskeleton coordination to desired coordination is affected by the stiffness level (1, 0.5, or 0) of the imposed coordination force field ($p = 0.002$). Post-hoc analysis reveals that there is a significant difference between the three levels. For 0-stiffness versus 1-stiffness we find $p = 0.004$, for 0-stiffness versus 0.5-stiffness, $p = 0.0394$, and for 0.5-stiffness versus 1-stiffness, $p = 0.0038$. Post-hoc analysis shows that for the target with a longer trajectory, at the slowest speed, there was a significant effect of the coordination control on reducing the task error (error at stiffness 0 was higher than error at stiffness 1, p = 0.014). Thus, for the slower, longer, and relatively more difficulty straight-line reaching movement, the coordination-based control could potentially decrease the task error.

A similar analysis in the conditions where participants 'push' the robot from the outside shows stronger effects of the force field on performance compared to the 'wear' cases. Specifically, there is a statistically significant effect of the coordination force field on the KCD of measured coordination behaviors ($p < 0.001$) with a significant difference between all three levels of stiffness ($p < 0.001$). There is an additional cross-effect of the target on the relative improvement (decrease) in KCD as the force field stiffness is increased. As the coordination force field stiffness is increased, the KCD becomes more similar for the two targets with a large error in the 0-stiffness case.

In addition to the joint-space coordination, we also evaluate the task space performance for each movement across all participants. The straight line between the home and target positions is defined in the task space using the reference data collected for each participant. Forward kinematics is used on the measured joint angle signals to calculate the true positions of the end effector during the test movements. The shortest distance to the straight-line path is calculated at each instant, averaged over the movement, and then normalized by the distance between the home and target positions. On average, there are no significant effects of the coordination levels (0, 0.5, and 1) on the task-space performance in the 'wear' case ($p > 0.05$), but a mild effect in the 'push' case. Together, the improved postural control for no loss (and potentially an improvement) in task-space accuracy suggests that participants are able to perform the task accurately in the presence of the corresponding joint-space force field while maintaining the desired joint coordination behaviors.

In the post-experiment survey, 6 of the 7 participants indicate a preference for modes with non-zero stiffness of the coordination control to perform the reaching task. Specifically, they find their task effort is reduced during these cases. One of the participants felt hindered rather than assisted by the coordination force field. 6 of 7 participants also report being able to perceive differences in the two non-zero levels of coordination stiffness. About half the participants prefer the reduced stiffness mode to the full stiffness mode. These observations suggest that in addition to ensuring joint coordination behaviors, the task-specific coordination field may provide task assistance depending on the stiffness of the force field and the individual's skill for the given task. More experiments with cognitive and motor load sensing (e.g. through muscle activity) are necessary to establish the assistive properties of this control mode.

IV. DISCUSSION

This paper implements and validates a control law, joint angle coordination control (JACC), that imposes postural coordination between the joints of a multi-dimensional robot through torque control while allowing for variable human-robot interaction. The presented control law is built by combining approaches presented in prior literature and implemented to ensure joint angle coordination of the exoskeleton as the wearer drives the robot's motion for a given task. The experimental analysis systematically tests the control law and demonstrates its robustness to various conditions. A human-subject study further establishes the feasibility of the JACC force field as a task environment that ensures joint coordination while allowing task completion under different forms of interaction between an individual and a robot. The experiments presented in this paper offer some key insights.

The first set of experiments testing the coordination of the robot under different coordination vectors and different levels of stiffness shows that the coordination force field effectively maintains the desired joint coordination behaviors. Further, by modulating the force field stiffness, we can set how rigidly the robot follows the desired coordination depending on the task application and to ensure wearer safety during the interaction. Testing with human subjects shows that the force field allows safe interaction between an individual and the exoskeleton both when the exoskeleton is worn and when it is pushed externally. The different speeds and forms of interaction demonstrate that the coordination force field can react appropriately no matter where or when the input is given by the human. Finally, the comparison between different levels of stiffness suggests that depending on the interaction mode ('Wear' or 'Push') or task goal the robot may need to impose the desired force field to different extents to cause an improvement in joint coordination. Specifically, we see that interactions in the 'Push' condition benefit from even a 0.5-stiffness field (decreased KCD compared to 0-stiffness) whereas those in the 'Wear' condition require the robot to impose the coordination with higher stiffness to see a significant improvement. This result can be explained by the robot's need to move both its joints as well as the wearer's body in the 'Wear' case whereas, in the 'Push' case, the robot only corrects its own joint behavior. The overarching conclusion of the analyses presented in this paper is that the coordination force field is effective and can constrain the joint coordination behaviors of the human-robot system during unstructured interactions.

Some key advantages of the joint-angle force field approach should be noted here. Crocher et al. [18] first presented the idea of using a force field to impose joint velocity coordination for exoskeleton-based training and rehabilitation. However, the authors impose coordination explicitly in the joint velocity space, and not the joint angle space. As a consequence, depending on the initial configuration and accumulation of errors over time, a wearer could move the exoskeleton through increasingly different joint angle coordination behaviors while maintaining joint velocity coordination. Our goal in this work is to instead impose joint angle coordination based on prior literature that suggests such coordinations are a representation of expert task-specific behaviors [3], [8]. Due to the joint angle coordination, our implementation of the JACC law inherently also coordinates the joint velocities. Our reference behavior (mean position and coordination vector) construction method further addresses the challenge of joint angle coordination control for different task movements. Vallery et al. [16] proposed a similar PCA-based approach for joint-angle coordination of a lower-limb exoskeleton control. However, the authors need to

define driving and driven joints, thus restricting the available interaction modes. Our application instead simultaneously coordinates all joints of the robot to maintain the desired coordination. This difference in implementation allows the robot to receive interaction input from the user at any joint or at multiple joints simultaneously while maintaining the desired coordination. Future work will compare the implementation of coordination-based control presented in this paper with existing methods. It should also be noted that this paper presents a proof-of-concept solution using a proportional impedance controller. Other forms of low-level control (such as proportional-derivative control) and mid-level control (besides impedance control) will be tested in future iterations.

Imposing postural coordination behaviors on a multi-dimensional robotic system may have several applications beyond exoskeleton control, such as in the control of teleoperated systems or collaborative robots. This paper provides an initial assessment of the feasibility of this method for human-exoskeleton interaction when there is uncertainty about how, where, and when the interaction will occur on the robot. However, further experimentation is necessary to assess how the human user perceives and benefits from the coordination force field. For example, although 6 of our 7 participants prefer the non-zero coordination modes to the 0 stiffness mode, one participant finds the coordination force field to be an impediment to their motion. A large-scale study with different types of dynamic tasks with varying levels of force field stiffness is necessary to assess how this mode of robot control affects humans in terms of cognitive and physical load during the interaction. The work presented in this manuscript represents a crucial first step in establishing the robustness and feasibility of coordinating a multi-dof exoskeleton's joint angles to enable comfortable unstructured human interactions for a given task goal.

ACKNOWLEDGMENT

The authors thank Paria Esmatloo, Saad Yousaf, and Anna Bucchieri for their advice on implementing and testing this control law. This work was carried out jointly by the ReNeu Robotics Lab and Learning Agents Research Group (LARG) at UT. Effort in the ReNeu Lab is supported, in part, by NSF (1941260, 2019704) and Facebook. LARG research is supported in part by NSF (CPS-1739964, IIS-1724157, NRI-1925082, CMMI-2019704), ONR (N00014-18-2243), FLI (RFP2-000), ARO (W911NF-19-2-0333), DARPA, Lockheed Martin, GM, and Bosch. Peter Stone serves as the Executive Director of Sony AI America and receives financial compensation. Ashish Deshpande serves as the Chief Research Officer for and has equity shares in Harmonic Bionics, a company that aims to commercialize the Harmony exoskeleton. The terms of these arrangements have been reviewed and approved by The University of Texas at Austin in accordance with its policy on objectivity in research.

REFERENCES

[1] Neville Hogan. Impedance control: An approach to manipulation. In *1984 American control conference*, pages 304–313. IEEE, 1984.

[2] Chad G Rose, Ashish D Deshpande, Jacob Carducci, and Jeremy D Brown. The road forward for upper-extremity rehabilitation robotics. *Current Opinion in Biomedical Engineering*, 19:100291, 2021.

[3] Till Bockemühl, Nikolaus F Troje, and Volker Dürr. Inter-joint coupling and joint angle synergies of human catching movements. *Human Movement Science*, 29(1):73–93, 2010.

[4] Sajida Khanafer, Heidi Sveistrup, Mindy F Levin, and Erin K Cressman. Age-related changes in upper limb coordination in a complex reaching task. *Experimental Brain Research*, pages 1–10, 2021.

[5] Bo Huang, Caihua Xiong, Wenbin Chen, Jiejunyi Liang, Bai-Yang Sun, and Xuan Gong. Common kinematic synergies of various human locomotor behaviours. *Royal Society open science*, 8(4):210161, 2021.

[6] Dingyi Pei, Tulay Adali, and Ramana Vinjamuri. Generalizability of hand kinematic synergies derived using independent component analysis. In *2021 43rd Annual International Conference of the IEEE Engineering in Medicine & Biology Society (EMBC)*, pages 621–624. IEEE, 2021.

[7] Bongsu Kim and Ashish D Deshpande. Controls for the shoulder mechanism of an upper-body exoskeleton for promoting scapulo-humeral rhythm. In *2015 IEEE International Conference on Rehabilitation Robotics (ICORR)*, pages 538–542. IEEE, 2015.

[8] Keya Ghonasgi, Reuth Mirsky, Adrian M Haith, Peter Stone, and Ashish D Deshpande. Quantifying changes in kinematic behavior of a human-exoskeleton interactive system. In *2022 IEEE/RSJ International Conference on Intelligent Robots and Systems (IROS)*. IEEE, 2022.

[9] Julio S Lora-Millan, Juan C Moreno, and Eduardo Rocon. Coordination between partial robotic exoskeletons and human gait: A comprehensive review on control strategies. *Frontiers in Bioengineering and Biotechnology*, 10:842294, 2022.

[10] Brahim Brahmi, Mohammad Habibur Rahman, and Maarouf Saad. Impedance learning adaptive super-twisting control of a robotic exoskeleton for physical human-robot interaction. *IET Cyber-Systems and Robotics*, 5(1):e12077, 2023.

[11] Paria Esmatloo and Ashish D Deshpande. The effects of emg-based classification and robot control method on user's neuromuscular effort during real-time assistive hand exoskeleton operation. In *2021 43rd Annual International Conference of the IEEE Engineering in Medicine & Biology Society (EMBC)*, pages 7515–7515. IEEE, 2021.

[12] Xiaofeng Xiong, Cao Danh Do, and Poramate Manoonpong. Learning-based multifunctional elbow exoskeleton control. *IEEE Transactions on Industrial Electronics*, 69(9):9216–9224, 2021.

[13] Keya Ghonasgi, Ana C de Oliveira, Anna Shafer, Chad G Rose, and Ashish D Deshpande. Estimating the effect of robotic intervention on elbow joint motion. In *2019 28th IEEE International Conference on Robot and Human Interactive Communication (RO-MAN)*, pages 1–6. IEEE, 2019.

[14] Ana C De Oliveira, James S Sulzer, and Ashish D Deshpande. Assessment of upper-extremity joint angles using harmony exoskeleton. *IEEE Transactions on Neural Systems and Rehabilitation Engineering*, 29:916–925, 2021.

[15] Elizabeth B Brokaw, Theresa Murray, Tobias Nef, and Peter S Lum. Retraining of interjoint arm coordination after stroke using robot-assisted time-independent functional training. *J Rehabil Res Dev*, 48(4):299–316, 2011.

[16] Heike Vallery, Ralf Ekkelenkamp, Martin Buss, and Herman van der Kooij. Complementary limb motion estimation based on interjoint coordination: experimental evaluation. In *2007 IEEE 10th International Conference on Rehabilitation Robotics*, pages 798–803. IEEE, 2007.

[17] Modar Hassan, Hideki Kadone, Tomoyuki Ueno, Kenji Suzuki, and Yoshiyuki Sankai. Feasibility study of wearable robot control based on upper and lower limbs synergies. In *2015 International Symposium on Micro-NanoMechatronics and Human Science (MHS)*, pages 1–6. IEEE, 2015.

[18] Vincent Crocher, Anis Sahbani, Johanna Robertson, Agnès Roby-Brami, and Guillaume Morel. Constraining upper limb synergies of hemiparetic patients using a robotic exoskeleton in the perspective of neuro-rehabilitation. *IEEE Transactions on Neural Systems and Rehabilitation Engineering*, 20(3):247–257, 2012.

[19] Bongsu Kim and Ashish D Deshpande. An upper-body rehabilitation exoskeleton Harmony with an anatomical shoulder mechanism: Design, modeling, control, and performance evaluation. *The International Journal of Robotics Research*, 36(4):414–435, 2017.